

Towards development of a nonlinear perturbation method for analysis of springing of ships

Y.L. Shao* and O.M. Faltinsen

Department of Marine Technology, NTNU and CeSOS, NTNU

Trondheim, NO-7491, Norway.

Shao.yanlin@ntnu.no and Odd.Faltinsen@ntnu.no (*Presenting author)

1. Introduction

A time domain method is employed to analyze interactions between waves and floating bodies. The nonlinear free surface conditions and body boundary conditions are satisfied based on the perturbation method up to 3rd order. The objective is to theoretically study springing of ships. Springing is a weakly nonlinear problem. The relevant wave lengths are short relative to the ship length. Thus, for the ship springing problem, from computational efficiency point of view, a perturbation method has its advantage compared with a fully nonlinear method.

2. Description of the method

The 1st, 2nd and 3rd order free surface conditions follow by introducing the perturbation expansions of velocity potential $\phi = \phi_1 + \phi_2 + \phi_3 + O(\varepsilon^4)$ and wave elevation $\eta = \eta_1 + \eta_2 + \eta_3 + O(\varepsilon^4)$:

$$\begin{cases} \eta_t^{(m)} = \phi_z^{(m)} - F_1^{(m)}, & \text{on } z=0 \\ \phi_t^{(1)} = -g \cdot \eta^{(1)} + F_2^{(1)}, & \text{on } z=0, \quad m=1,2,3 \end{cases}$$

Where $F_1^{(1)} = 0$; $F_2^{(1)} = 0$;

$$F_1^{(2)} = -\phi_x^{(1)} \eta_x^{(1)} - \eta^{(1)} \phi_{xx}^{(1)};$$

$$F_2^{(2)} = -\frac{1}{2} |\nabla \phi^{(1)}|^2 - \eta^{(1)} \phi_{zt}^{(1)}$$

$$F_1^{(3)} = -\phi_x^{(1)} \eta_x^{(2)} - \phi_x^{(2)} \eta_x^{(1)} - \eta^{(1)} \phi_{xx}^{(2)} - \eta^{(1)} \eta_x^{(1)} \phi_{zx}^{(1)} - \eta^{(2)} \phi_{xx}^{(1)} - 0.5(\eta^{(1)})^2 \phi_{zxx}^{(1)}$$

$$F_2^{(3)} = -\nabla \phi^{(1)} \cdot \nabla \phi^{(2)} - \eta^{(1)} \phi_{zt}^{(2)} - \eta^{(1)} \nabla \phi^{(1)} \cdot \nabla \phi_z^{(1)} - \eta^{(2)} \phi_{zt}^{(1)} + 0.5(\eta^{(1)})^2 \phi_{lxx}^{(1)}$$

The small parameter ε here is a measure of the wave slope. A 2D numerical wave tank is considered. At each time step, boundary element method (BEM) is adopted to solve the boundary value problem (BVP) for the velocity potential ϕ

and its time derivative ϕ_t . Panels are distributed along the body surface S_b , free surface S_f , left vertical wall S_{w1} , right vertical wall S_{w2} and the bottom S_0 . (See fig.1). The variation of ϕ (or ϕ_t) and ϕ_n (or ϕ_{tn}) over each element are assumed linearly varying. The continuity condition of ϕ (or ϕ_t) at the intersection points of different boundaries is enforced. Fourth order Runge-Kutta method is applied to update ϕ and η on the free surface for the next time step.

The formulation of body boundary condition for ϕ follows that of Ogilvie (1983), while the body boundary condition for ϕ_t is based on Wu (1998).

Similar to Clement (1996), a coupling of a numerical beach and a piston-like absorbing boundary condition (PABC) is applied to absorb outgoing waves. The numerical beach used here is the same as that of Greco (2001). In order to obtain PABC at each time step, we solve the problem like solving the response of a floating body in waves.

3. Verification of the method

The accuracy of the numerical method is an important issue. With the purpose of verification, the free oscillations in a tank, the forced oscillations (wavemaker problem) in a tank, and the nonlinear diffraction and forced oscillations of a horizontal cylinder are studied. The results are presented up to 2nd order and comparisons between the analytical results and the experimental results are made.

Cointe et al. (1988) studied two cases of nonlinear transient wave in a rectangular tank. One case is the free oscillation problem, in which an initial displacement is given to the free surface. In the simulation, we set $L=1.0\text{m}$, $h=0.2\text{m}$ and $z_0=0.02\cos(\pi x)$ m, where L is the length of the tank, h is the water depth and z_0 is the initial displacement of free surface. Fig.2a and Fig.2b show the numerical results of 1st order and 2nd order wave elevation at

$x=L/8$, together with the corresponding analytical results at that point. The agreement between the numerical results and the analytical solution is very encouraging.

The forced oscillation (wave maker problem) is also investigated by Cointe et al. (1988). The motion is prescribed on S_{w1} , while S_{w2} is fixed. As a useful test to check the accuracy of numerical results, Cointe et al. (1988) suggest the following equation to control the mass conservation at second-order:

$$\int_0^L \eta^{(2)}(x,t) dx = l_1(t) \eta^{(1)}(0,t)$$

Here, L is the length of the tank; $\eta^{(1)}(0,t)$ is the 1st order wave elevation on S_{w1} ; $\eta^{(2)}(x,t)$ is the 2nd order wave elevation; $l_1(t) = F(t) \cdot A_{w1} \sin(\omega t)$ is the displacement of S_{w1} . $F(t)$ is the ramp function applied over the first 2 wave periods. A_{w1} is the amplitude of the displacement of S_{w1} .

Mass conservation is checked at the end of the third period. The results for first-order and second-order mass check are presented in Fig.3, showing the convergence with the increasing number of elements on the free surface.

Another good way of generating waves in a numerical tank is to feed a theoretical particle velocity profile along the vertical input boundary. This method has been adopted by Koo and Kim (2004) in their fully nonlinear wave tanks, and by Skourup (1996) in 2nd order wave tank. However, we must be careful with the mass transport due to the boundary condition that is used. One would expect the increase of mass all the time without a damping zone mechanism that can take mass out of the system. The rate of mass transport is given by Dean and Dalrymple (1991) as $\rho g a^2 k / (2\sigma)$, where ρ is the density of water, σ is the wave frequency, g is gravity acceleration and k is the wave number. As shown in Fig.4, the rate of mass transport observed in the 2nd order simulation agrees well with that given by Dean and Dalrymple (1991). Note that the mass transport shown in the figure is non-dimensional, and the offset of the two curves is due to the ramp function which is used to give a smooth start of the flow.

Isaacson and Ng (1993) studied the forced oscillation of a horizontal cylinder in deep water. Their method was based on a constant element

method with implicit 2nd order Adam-Moulton for the time integration of free surface conditions. ϕ_t was derived by a finite difference method.

In the literature, there are two ways to get the 2nd order force acting on the body, i.e. the direct integration method (Pinkster and Oortmerssen, 1977) and indirect method based on Green's 2nd identity (Faltinsen, 1976). In the former method, one has to solve the 2nd order problem and integrate the pressure on the body surface. In the latter method, instead of solving the 2nd order problem, we can obtain the 2nd order force by using the boundary conditions and solutions of the linear problems. In this paper, we introduce two artificial velocity potentials and use the indirect method as a tool to check the 2nd order numerical results.

The artificial velocity potentials ψ_i ($i=1, 2$) introduced are similar to Wu and Taylor (2003). ψ_i satisfies the Laplace equation, $\psi_i = 0$ on $z=0$, $\frac{\partial \psi_i}{\partial n} = n_i$ on the mean

position of body surface, $\psi_i \rightarrow 0$ as $z \rightarrow -\infty$ and the radiation condition. Green's 2nd identity leads to

$$\int_{S_b + S_f + S_\infty} \left(\phi_t^{(2)} \frac{\partial \psi_i}{\partial n} - \psi_i \frac{\partial \phi_t^{(2)}}{\partial n} \right) ds = 0,$$

where $\phi_t^{(2)}$ is the time derivative of the second order velocity potential $\phi^{(2)}$, n is the unit normal to the surface, defined as positive pointing out of the fluid domain.

Using the condition for $\phi_t^{(2)}$ at infinity and the free surface condition for ψ_i , we obtain

$$\begin{aligned} F_i^{(2)} &= -\rho \int_{S_b} \phi_t^{(2)} n_i ds = -\rho \int_{S_b} \phi_t^{(2)} \frac{\partial \psi_i}{\partial n} ds \\ &= -\rho \left[\int_{S_b} \psi_i \frac{\partial \phi_t^{(2)}}{\partial n} ds - \int_{S_f} \phi_t^{(2)} \frac{\partial \psi_i}{\partial n} ds \right] \\ &= -\rho \left[\int_{S_b} \psi_i \frac{\partial \phi_t^{(2)}}{\partial n} ds - \int_{S_f} \phi_t^{(2)} \frac{\partial \psi_i}{\partial n} ds + \int_{S_f} \psi_i \frac{\partial \phi_t^{(2)}}{\partial n} ds \right] \\ &= -\rho \left[\int_{S_b} \psi_i \frac{\partial \phi_t^{(2)}}{\partial n} ds - \int_{S_f} \phi_t^{(2)} \frac{\partial \psi_i}{\partial z} ds \right] \end{aligned}$$

The analytical solution for ψ_i for a half circular cylinder has been derived, by taking an image of the body and solving the integral equation directly. The expression for $\frac{\partial \psi_i}{\partial z}$ on the free surface is found to be

$$\frac{\partial \psi_i}{\partial z} = \begin{cases} -\frac{2}{\pi} \left[\frac{1}{\gamma} + \frac{1}{2} \ln \left| \frac{\gamma-1}{\gamma+1} \right| \left(1 + \frac{1}{\gamma^2} \right) \right]; & i=1 \\ -\frac{1}{\gamma^2}; & i=2 \end{cases}$$

Here $\gamma = \frac{x}{R}$, R is the radius of the cylinder, x is defined as in Fig.5.

We note that $\frac{\partial \psi_1}{\partial z}$ has a logarithmic singularity at the intersection point of the free surface and the body. Consequently, ψ_1 is also singular at the intersection point. However, the singularity itself doesn't matter because the integration of the singularity over an infinitesimal area is finite. Fig.6a shows the amplitude of 2nd order oscillatory forces due to 2nd order velocity potential $\phi^{(2)}$. The agreement between the results of direct integration method and that of the indirect method is excellent, indicating the accuracy of the 2nd order solution. In Fig.6b and Fig.6c, we also present the amplitude of the total oscillatory forces compared with the theoretical and experimental results of Yamashita (1977) and Kyojuka (1982).

The fixed horizontal cylinder in deep water waves was studied by Isaacson and Cheung (1991). The wave field is separated to the known incident wave ϕ_i and the unknown scattered wave ϕ_d . The second order solution is again checked by Green's 2nd identity. (See Fig.7a). The agreement between the direct method and method based on Green's 2nd identity is fairly good. The total 2nd order horizontal force compared with theoretical and experimental results by Kyojuka (1982) is shown in Fig.7b, while the horizontal mean drift force is checked by Maruo's formula, as shown in Fig.7c.

4. Future work

Verification work is being carried out for 3rd order results in two-dimensional problems. This will be done first by considering a 3rd order problem where an analytical solution is possible by imposing an artificial body boundary condition. Details will be presented at the conference. In order to investigate ship springing, the method will be generalized to three dimensions with the effect of forward speed.

5. Reference

- 1) Clement, A., 1996. Coupling of two absorbing boundary conditions for 2D time-domain simulations of free surface gravity waves. *J. Comp. Phys.* 126, pp. 139–151.
- 2) Cointe, R., Molin, B., Nays, P., 1988. Nonlinear and second-order transient waves in a rectangular tank. In: Proc. behavior of offshore structural systems conf. 1988.
- 3) Dean, R.G., Dalrymple, R.A, 1991. *Water Wave Mechanics for Engineers and Scientists*, World Scientific.
- 4) Faltinsen, O.M., 1976. Slow-drift excitation of a ship in irregular beam sea waves. DNV Report, No.76-083.
- 5) Greco, M., 2001. A two-dimensional study of green-water loading. PhD thesis, Dept of Marine Technology, NTNU, Trondheim, Norway.
- 6) Isaacson, M., Cheung, K.F., 1991. Second order wave diffraction around two-dimensional bodied by time-domain method. *Applied Ocean Research* 13, 175-186.
- 7) Isaacson, M., Ng, J.Y.T., 1993. Time-domain second-order wave radiation in two dimensions. *Journal of ship Research*. Vol.37, No. 1, pp. 25-33.
- 8) Koo, W., Kim, M., 2004. Freely floating body simulation by a 2D fully nonlinear numerical wave tank. *Ocean Eng.* v31. 2011-2046.
- 9) Kyojuka, Y., 1982. Experimental study on Second order forces acting on cylinder body in waves. *Proceedings, 14th Symposim on Naval Hydrodynamics*, Ann Arbor, Mich., 319-382.
- 10) Ogilvie, T.F., 1983. Second-order hydrodynamic effects on ocean platforms. *Proc. Intl. Workshop Ship and Platform Motions*, pp. 205–265.
- 11) Pinkster, J.A., van Oortmerssen, G., 1977. Computation of the first and second order wave forces on oscillating bodies in regular waves, *Proc. 2nd Internat. Conf. on Numerical Ship Hydrodynamics*, pp. 136-159.
- 12) Skourup, J., 1996. Active Absorption in a Numerical Wave Tank. *Proc., Sixth International Offshore and Polar Engineering Conference*, Los Angeles, CA, 3, pp. 31–38.
- 13) Wu, G. X., 1998. Hydrodynamic force on a rigid body during impact with liquid. *J. Fluids Struct.*, 12, pp. 549–559.
- 14) Wu, G.X., Taylor, R.E., 2003. The coupled finite element and boundary element analysis of nonlinear interactions between waves and bodies. *Ocean Engineering*, 30, 387-400.

15) Yamashita, S. 1977. Calculations of the hydrodynamic forces acting upon thin cylinders oscillating vertically with large amplitude. Journal of the Society of Naval Architects of Japan, 141, 61-69.

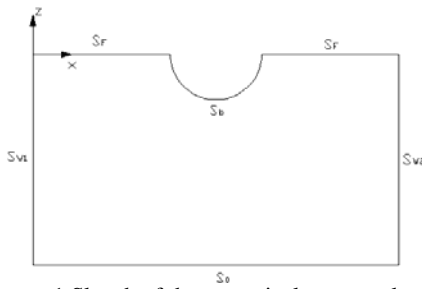


Fig.1 Sketch of the numerical wave tank with the presence of a body.

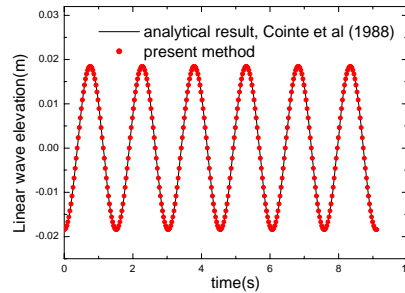


Fig.2a 1st order component of wave elevation at $x=L/8$

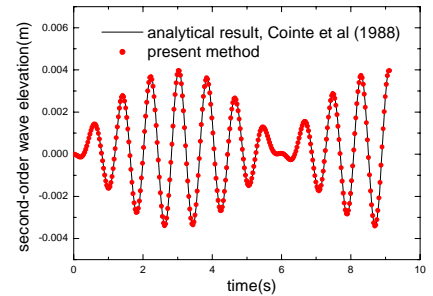


Fig.2b 2nd order component of wave elevation at $x=L/8$

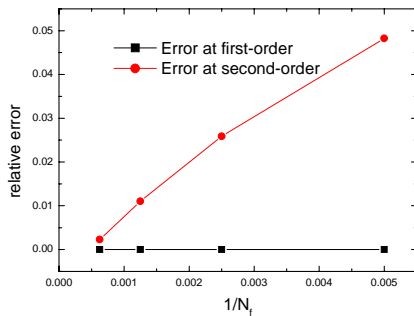


Fig.3 The relative error of the mass conservation.

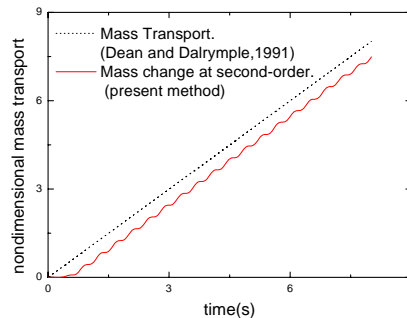


Fig.4 The mass transport into the tank

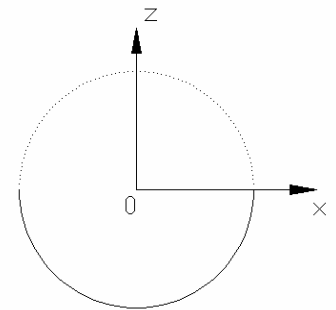


Fig.5 Definition of the coordinate for the problem of ψ_i

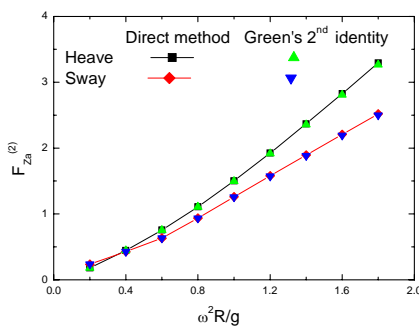


Fig.6a Amplitude of 2nd order oscillatory force due to $\phi^{(2)}$ in the forced oscillation of the cylinder.

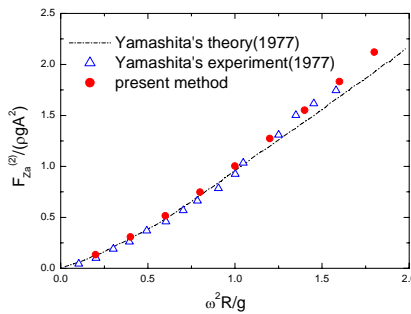


Fig.6b Amplitude of $F_z^{(2)}$ force in heave motion. $F_z^{(2)}$ is the total 2nd order oscillatory force in vertical direction.

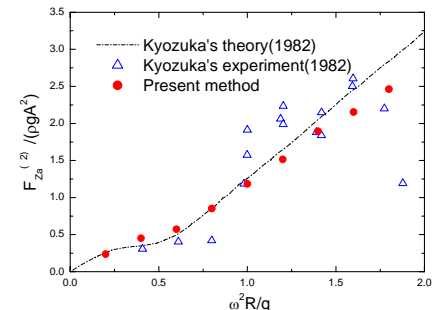


Fig.6c Amplitude of $F_z^{(2)}$ force in sway. $F_z^{(2)}$ is the total 2nd order oscillatory force in vertical direction.

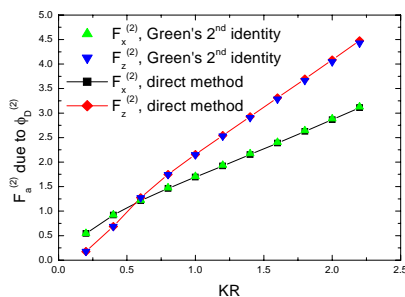


Fig.7a Amplitude of 2nd order oscillatory force due to $\phi_d^{(2)}$ when the cylinder is fixed with incident wave.

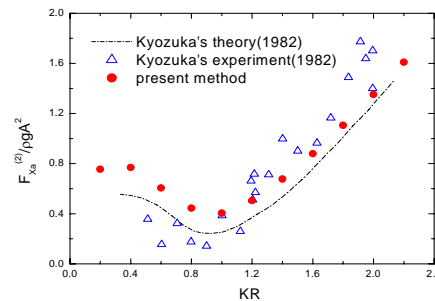


Fig.7b Amplitude of $F_x^{(2)}$ on a fixed horizontal cylinder with incident wave.

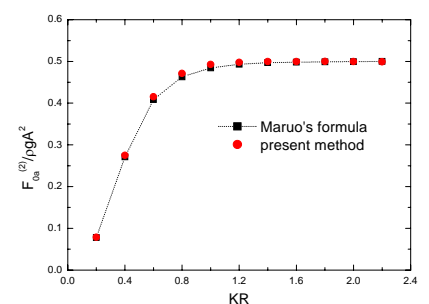


Fig.7c Horizontal mean drift force on a fixed horizontal cylinder with incident wave.